Twenty-Fifth Symposium (International) on Combustion/The Combustion Institute, 1994/pp. 353–361

ANALYSIS OF DROPLET ARRIVAL STATISTICS IN A PRESSURE-ATOMIZED SPRAY FLAME

J. T. HODGES AND C. PRESSER
Chemical Science and Technology Laboratory
National Institute of Standards and Technology
Gaithersburg, MD 20899, USA
A. K. GUPTA
Department of Mechanical Engineering
University of Maryland
College Park, MD 20742, USA
AND
C. T. AVEDISIAN
Sibley School of Mechanical and Aerospace Engineering
Cornell University
Ithaca, NY 14853, USA

The statistical behavior of droplets in a kerosene pressure-atomized spray was investigated under swirling and burning conditions. This case was studied in order to better understand individual droplet transport processes downstream of the fuel spray flame. A two-component phase-Doppler particle sizing system was employed to provide information on the droplet size and velocity distributions as well as interarrival-time statistics. Time-resolved information is presented on the instantaneous values of diameter, and the respective axial and radial velocity components. The results provide some evidence of nonsteady interarrival-time statistics (associated with droplet clustering) immediately downstream of the fuel nozzle and at radial coordinates near the center of the spray. This unsteady statistical behavior was most prominent within the shear layer formed near the inner spray boundary. Decomposition of the results into size classes indicated that clustering (attributed to entrainment by recirculating gases) occurred only for the smallest droplets, 0–20 μm in diameter. For larger droplets, analysis on the random nature of the spray process revealed that droplet transport generally follows steady Poisson statistics. Furthermore, the information provided here shows that size-class decomposition is important in the analysis of spray behavior.

Introduction

Improved understanding of spray combustion phenomena requires a detailed knowledge of the interaction between the droplets and the surrounding chemically reacting flow field. Therefore, novel strategies that address optimization of fuel/air mixing processes can lead to increased combustion efficiency and reduced emission of unburnt fuel into the surrounding environment. The importance of matching the fuel spray pattern with the associated aerodynamic flow field has been recognized through the direct application of laser sheet photography. Studies have shown that droplets pass through the flame sheet relatively unburnt when using commercially available atomizers [1]. Information dealing with the effect of the gas flow field (both mean and fluctuating quantities) on the trajectory of individual droplets of various sizes is critical to determine the dispersion of droplets within the surrounding air stream.

Recent developments with phase-Doppler interferometry (PDI) have allowed simultaneous measurement of both size and velocity distributions, and time-resolved information [2]. The effect of aerodynamic turbulence on droplet dispersion can be obtained with PDI in different environments, including swirling and burning droplet-laden streams. Reitz [3] found that droplet mean and fluctuating velocities were close to that of the gas stream for situations where the droplet-size–velocity correlation coefficient was low. This occurred in regions of the spray where the relative velocity between the droplets and gas stream was small, for example, in downstream regions and in the center of the spray. Edwards and Rudoff [4] found that groups of droplets of specified size range have different velocities, and that mean velocity decreases with smaller droplet size class. The droplet velocities associated with the smaller-sized droplets were found to merge smoothly into the gas-phase velocity. The velocity of the gas remained be-

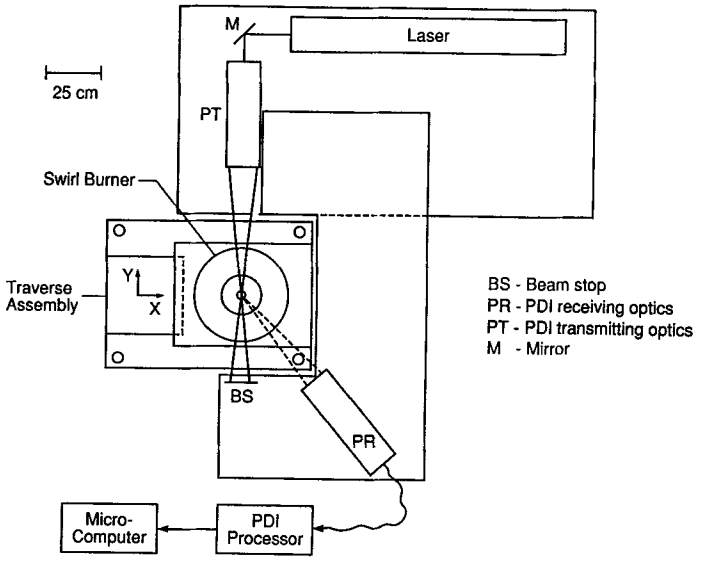

FIG. 1. Schematic of the experimental droplet velocity/sizing apparatus.

low that of the smallest droplet size class throughout each radial profile except near the dense spray boundary (in the near-injector region) where sensitivity to the smallest droplet sizes was lost. Bulzan et al. [5] have found both experimentally and numerically that the fluctuating radial gas-phase velocity is significantly lower than the axial component in a downward-facing air-assisted water spray. The magnitude of the radial fluctuations remains smaller than the axial component with increasing axial position, although the flow becomes more isotropic.

The focus of this investigation was to provide time-resolved information on the instantaneous droplet velocities and interarrival-time statistics as correlated with droplet size and spray position. Data are presented for a swirling kerosene spray flame, as opposed to earlier studies under nonburning conditions [6,7]. This study provides further insights pertinent to a better understanding of droplet interaction with the surrounding air stream.

Experimental Arrangement

Spray Combustor Facility:

Experiments carried out in the spray combustion facility (SCF) simulate operating conditions found in practical combustion systems (see Fig. 1). The swirl burner includes a moveable-vane swirl generator with a 12-vane cascade; the vanes rotate simultaneously in order to impart the desired degree of swirl intensity (both positive and negative) to the combustion air flow [8]. The pressure-jet nozzle used in the present study was nominally operated at a fuel flow rate of 3.2 kg/h (line pressure at about 6.89 kPa). The combustion air, supplied to the burner via a 101-mm-diameter pipe surrounding the fuel nozzle, was nominally set at 64.3 kg/h. This provided good flame stability at an overall input fuel/air equivalence ratio of 0.75. Further details of the experimental facility are presented in Ref. 8.

The unconfined spray is injected vertically upward from the nozzle exit, located at the burner exit. A stepper-motor–controlled spray assembly traversing system allows movement in both the vertical and horizontal planes so that highly resolved spatial profiles can be obtained within the spray flame. The optical setup is fixed while the burner spray assembly is moved. In this fashion, radial profiles of the spray properties are obtained at different axial positions.

Measurement of Droplet Size, Velocity, and Time of Arrival

A two-channel phase-Doppler interferometer (PDI) is used to obtain droplet time of arrival, droplet size, and velocity data. By "time of arrival" is meant the time relative to the start of data acquisition at which a given droplet is detected. Measurements were repeated at several selected positions to ensure a repeatability that was generally better than 5% near the spray boundary.

Results and Discussion

Size/Velocity Distributions and Time of Arrival:

Two positions were selected to illustrate the behavior of the individual droplets, one at the centerline and the second near the spray boundary (i.e., the

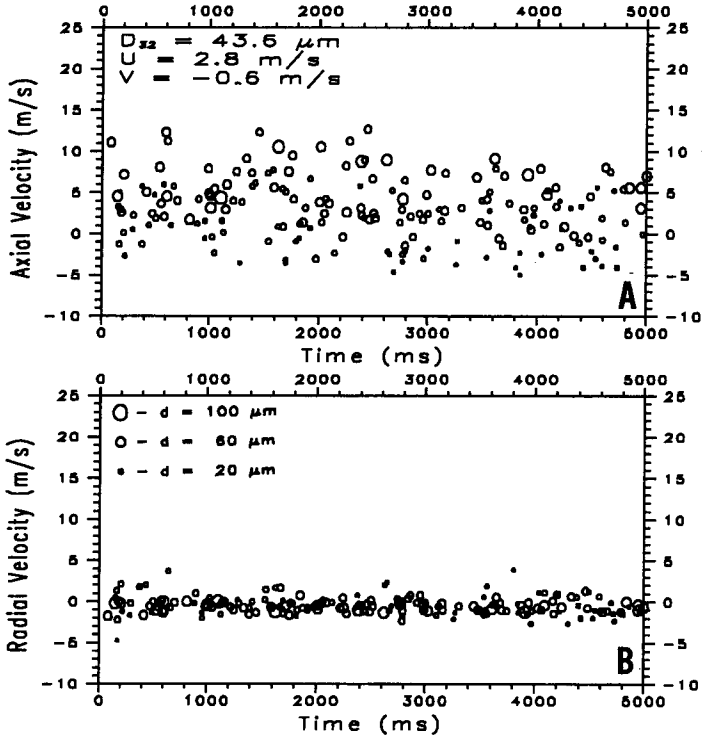

FIG. 2. Time history of droplet (a) axial and (b) radial velocity at $r = 0$ and $z = 10$ mm. Velocity time histories are coded to represent change in droplet diameter.

position radially outward near the outer edge of the spray where droplet size is maximized). Results are presented in Figs. 2 and 3 at an axial position, z, of 10.0 mm and for radial positions, r, of 0 and 10.2 mm, respectively. Each figure includes the droplet axial and radial velocity time of arrival (note the difference in scales for time in Figs. 2 and 3). The data points in each figure are also coded to represent the droplet diameter (for $1 \leq D \leq 100\ \mu$m, see scale in frame B of each figure). At $r = 0$ (see Fig. 2a), the presence of both negative and positive droplet axial velocities is attributed to recirculated droplets and to droplets injected directly from the nozzle, respectively. Near the spray boundary (at $r = 10.2$ mm), the results indicate the presence of droplets originating solely from the nozzle exit (i.e., only positive axial velocities are revealed in Fig. 3a). In a previous study [9], it was shown that a bimodal size distribution is detected near the spray centerline and is attributed to the formation of a recirculation zone (consisting of mostly smaller-sized droplets) downstream of the nozzle. These results are of interest to burning studies since smaller droplets found under these conditions are captured by the gaseous recirculation pattern and transported upstream toward the nozzle. Under nonburning conditions [7], the strength of the central toroidal recirculation zone is much larger and stronger than that which develops for burning conditions. Although the recirculation zone in the burning spray is relatively weak, smaller droplets are transported upstream along the spray centerline and subsequently swept into the droplet mainstream along the spray boundary. At downstream positions, data were not obtained near the spray centerline because of the low data rates that were associated with the dramatically reduced droplet concentrations. Near the spray boundary, the size and velocity distributions were essentially the same as those at $z = 10$ mm because of the lack of axial droplet deceleration [10]. This lack of deceleration is attributed to the increased gas-phase volumetric flow rate that is induced by the combustion process.

The diameter of individual droplets corresponding to each droplet arrival time is shown in Figs. 2 and 3. The figures indicate that the droplets (i.e., both large and small) randomly enter the measurement volume. Spectral density analysis carried out with time-of-arrival data obtained during a previous investigation [11] did not indicate the presence of any dominant frequencies in the spray at $z \geq 10$ mm. High-speed cinematography has shown the presence of a high-frequency pulsation (at approximately 1 kHz) in the spray jet and apparent clustering of droplets immediately downstream of the nozzle ($z < 10$ mm), which is attributed to liquid sheet breakup [8]. This pulsation appears to decay rapidly within a few millimeters of the nozzle exit.

At the spray centerline, the data rate is much lower than detected near the spray boundary (see Figs. 2 and 3). Both swirl and combustion act to reduce the

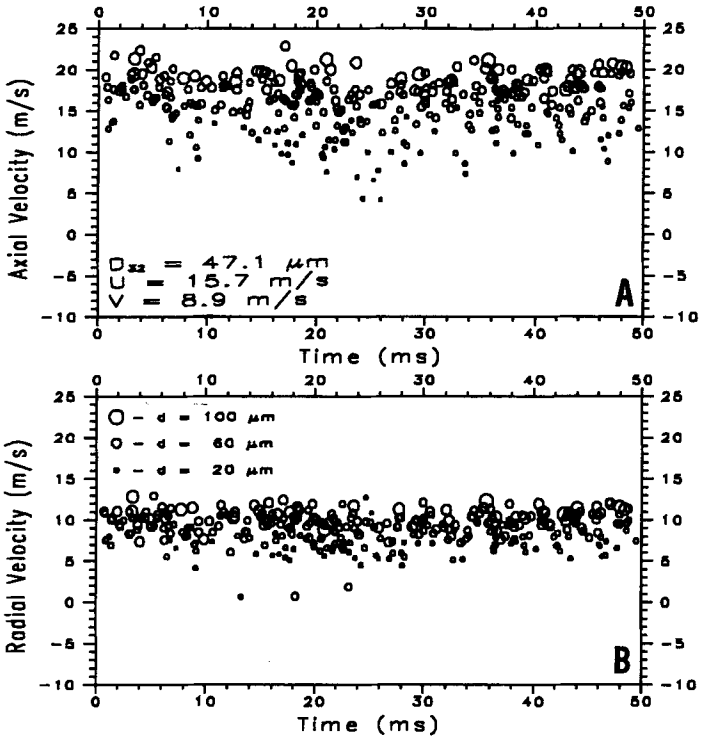

FIG. 3. Time history of droplet (a) axial and (b) radial velocity at r = 10.2 mm and z = 10 mm. Velocity time histories are coded to represent change in droplet diameter.

droplet concentration and therefore the data rate. The larger droplets that are fewer in number often pass with less frequency through the measurement volume at high velocity. At both radial positions, there is an obvious trend for the axial velocity sequence; viz., transport of the smaller droplets is at lower axial velocities while the larger droplets move at higher velocities. The radial velocity sequences presented in Figs. 2b and 3b indicate less correlation between size and velocity as compared with the axial velocity results.

Droplet Interarrival Statistics:

The time-of-arrival PDI data shown in Figs. 2 and 3 indicate that droplets pass through the probe volume in a random fashion (the term *random* is used in the sense that, at any instant, the detection of a droplet cannot be predicted a priori). A quantitative interpretation of single-point, time-resolved spray data can be carried out based on the recently developed ideal spray theory of Edwards and Marx [12,13]. In this theory, the ideal spray, which is defined as a discrete stochastic process, is comprised of droplets (treated as noninteracting point particles) randomly passing through a given point in space. The droplet flux within an ideal spray, in general, follows either homogeneous (steady in time) or inhomogeneous Poisson statistics. In a statistical sense, the ideal spray is defined completely by knowledge of the time-dependent process intensity function, $\lambda(t)$, where t represents time and for which the intensity function is equivalent to the particle arrival rate. Consequently, the probability of realizing a given set of droplet interarrival times depends solely on the intensity function. Note that a time-of-arrival sequence of $M + 1$ droplets constitutes a realization of M interarrival times, where the interarrival time is the difference in arrival time between successive droplets.

The functional form of $\lambda(t)$ can be used to classify the spray into three basic types [13]: (1) steady, (2) unsteady-deterministic, or (3) unsteady-random, corresponding to situations for which the intensity function is (1) independent of time, (2) time-dependent and deterministic, or (3) time-dependent and random, respectively. If the intensity function is time invariant, i.e., steady, then the spray follows homogeneous Poisson statistics.

Any ordering of the spray will influence the intensity function and therefore affect the droplet interarrival (or occurrence) statistics. In an actual spray, unsteady statistics can exist because of ordering and clustering of droplets as, for example, a result of aerodynamic effects or by periodicity generated by system pulsations. Statistical analysis of the occurrence events can therefore provide information regarding the nature of randomness of the spray field.

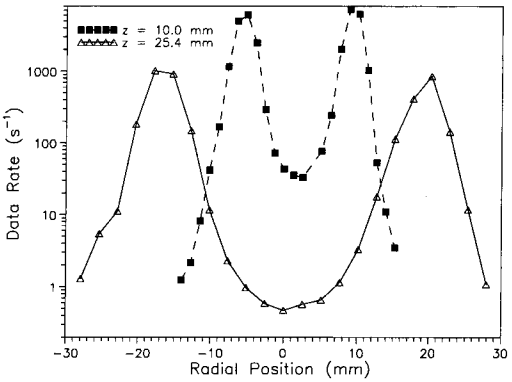

FIG. 4. Variation of phase-Doppler data rate with radial position at $z = 10$ mm and $z = 25.4$ mm.

The intensity, which represents the droplet arrival rate at a given point within the spray, is equivalent to the droplet flux (units, s^{-1}) passing through the measurement volume. Its magnitude is proportional to the local droplet concentration and velocity distribution integrated over the projected area of the probe volume. The actual measured intensity, $\lambda_m(t)$, also known as the data rate, is proportional to the fraction of droplet arrival events, β, which yield a validated response by the measurement apparatus, i.e., $\lambda_m(t) = \beta\lambda(t)$. At very high system gain, the validation fraction will tend to decrease as a consequence of increased detector signal noise. In this study, the gain was varied with radial position in order to accommodate changes in droplet mean diameter. At coordinates corresponding to relatively high gain and small mean droplet diameter, the validation fraction, as indicated by the PDI, was low, with $\beta \sim (0.2\text{–}0.4)$. Conversely, within the spray boundary, where the droplet mean diameter was large, system gain was reduced, and validation fraction was of the order $\beta \sim (0.6\text{–}0.8)$. It is important to note that, although the validation fraction alters the magnitude of the data rate, the shape of the interarrival-time distribution function is unaffected.

The expected value of the intensity, $\langle\lambda\rangle$, is equivalent to the average particle arrival rate and can be determined by dividing the number of interparticle events, M, by a sufficiently long time interval over which the particle events are observed to occur. Two radial profiles of the data rate, $\lambda_m = \beta\langle\lambda\rangle$, corresponding to $z = 10$ and 25.4 mm, are presented in Fig. 4. The profiles are nearly symmetric about the spray centerline, with somewhat increased asymmetry for $z = 10$ mm. Near the spray centerline, both profiles exhibit pronounced minima resulting from the relatively low droplet concentration. Conversely, the measured peak intensity of both profiles occurs near the spray boundary, with a maximum arrival rate at $z = 10$ mm of approximately 8×10^3 s^{-1}. At $z = 25.4$ mm, the radial spread of the spray is more than twice that of the $z = 10$ mm profile. Along the spray axis, the depleted droplet concentration yields a centerline data rate that is over three orders of magnitude less than the peak value of 10^3 s^{-1} near the spray boundary. One notes that the radial profile of the intensity, $\langle\lambda(r)\rangle$, differs in magnitude, and slightly in form, from the data rate, $\lambda_m(r)$, because of the spatial variation of the validation fraction, $\beta(r)$. With regard to $\langle\lambda(r)\rangle$, the reduction in the validation fraction at the spray centerline (relative to the peak value near the spray boundary) increases the magnitudes of the central minima of Fig. 4 by a factor of approximately 3.

In order to justify the dilute spray assumption (explicitly assumed in the model of an ideal spray), the ratio of droplet diameter, D, to interparticle separation, Λ, is estimated using values based on measured spray properties. For characteristic ratios, $D/\Lambda << 1$, it is expected that the average interparticle separation may be considered large enough so that the dilute spray approximation can be justified. The interparticle separation can be approximated by the cube root of the reciprocal of droplet number density, i.e., $\Lambda \sim N^{-1/3}$. The smallest interparticle separation was found to occur near the nozzle exit and spray boundary, where the maximum droplet number density and diameter were approximately 3500 particles cm^{-3} and 80 μm, respectively. Based on these values, it was estimated that this characteristic ratio was small, $D/\Lambda \sim 0.12$. This result shows that, on the average, the most dense region of the spray was relatively dilute although it is recognized that, at any given time, the ratio D/Λ can be much higher as a result of the occurrence of random fluctuations in interparticle spacing.

The occurrence statistics of the spray were quantified via the normalized interarrival-time-distribution histogram, $H(\tau_j,\Delta\tau_j)$, which was obtained from the phase-Doppler data. This histogram can be generated by counting the number of interparticle arrival times occurring within the jth time bin τ_j of width $\Delta\tau_j$, as:

$$H(\tau_j,\Delta\tau_j) = \frac{1}{M\Delta\tau_j} \cdot \text{count}[\tau_j - \Delta\tau_j/2 \le \tau < \tau_j + \Delta\tau_j/2] \quad (1)$$

where τ represents a measured arrival time and M is the total number of interarrival events. The interarrival probability density function, $h(\tau)$, which is a continuous function describing a process of infinite duration, is defined in terms of $H(\tau_j,\Delta\tau_j)$. In the limit of infinite sample population, M, and infinitesimal bin width, $\Delta\tau_j$, namely ($\lim \Delta\tau_j \to 0$, $M \to \infty$), then $H(\tau_j,\Delta\tau_j) \to h(\tau)$. Therefore, given a finite

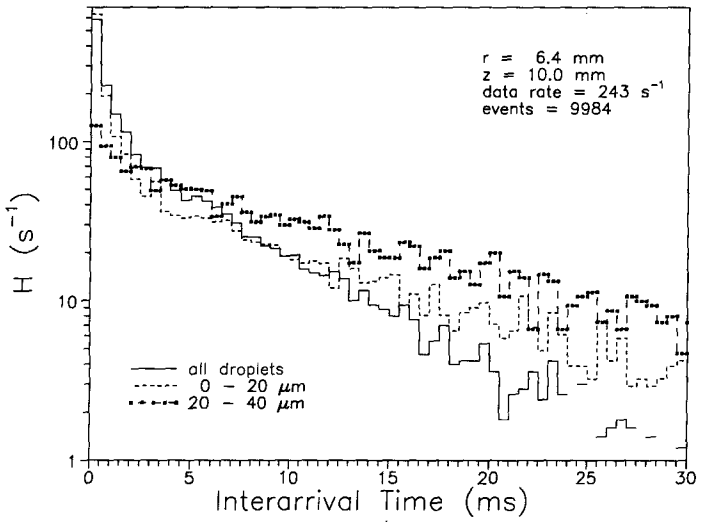

FIG. 5. Probability distribution of interarrival times for different diameter-based size classes at z = 10 mm and r = 6.4 mm.

sample population, $H(\tau_j,\Delta\tau_j)$ is an approximation to $h(\tau)$.

For a steady Poisson process, the interarrival probability density function, $h(\tau)$, is well known and is given in terms of the interarrival time, τ, and intensity, λ, as [14]

$$h(\tau) = \lambda e^{-\lambda\tau} \tag{2}$$

so that, for a steady spray, a plot of $\ln[h(\tau)]$ vs τ will have a constant slope equal to λ and intercept equal to $\ln(\lambda)$.

Given a sufficiently large sample size and exponential distribution characteristic of a steady spray, the relationship between $\ln[H]$ and τ will approach linearity. With this idea in mind, several representative normalized interarrival-time histograms, $H(\tau_j, \Delta\tau_j)$, were calculated from the time-series data (obtained at selected positions in the spray flame) and compared with the theoretical behavior of a statistically steady spray. For example, this statistical analysis was carried out for data obtained at z = 10 mm and r = 6.4 mm (see Fig. 5). At this position, recirculated droplets begin to interact with the droplets that are transported downstream directly from the nozzle. Three interarrival-time histograms were constructed from the following three diameter classes: (a) all sizes, (b) 0–20 μm , and (c) 20–40 μm. Nearly 10^4 particles were sampled over class (a), with about 6000 in class (b) and 3000 in class (c). At this position, the average measured intensity (over all size classes) was 243 s^{-1}, and the droplet number density was 250 particles cm^{-3}.

For the pair of curves corresponding to classes (a) and (b) in Fig. 5, there is a statistically significant departure from linearity at short interarrival times. Note that, since class (b) comprises nearly 60% of the entire population, the histogram for class (a) is heavily weighted by that class. This accounts for the similarity of the histograms for classes (a) and (b). For class (b), there is a relatively abrupt change in the magnitude of the histogram slope (intensity) that occurs at an interarrival time of approximately 3.5 ms. This result indicates an unsteadiness in the arrival-time statistics for the 0–20-μm-diameter size class at the coordinates z = 10 mm and r = 6.4 mm. This behavior persists as one moves toward the spray centerline where there is an abundance of smaller droplets. In contrast, the histogram for class (c) shown in Fig. 5 conforms more closely to the exponential distribution given by Eq. (2), thus revealing that the largest droplets exhibit nearly steady interarrival-time statistics. Near the spray boundary at z = 10 mm and r = 10.2 mm, the histogram (over all size classes) is consistent with steady Poisson statistics. At this location, the spray is relatively dense and is comprised mainly of larger droplets ($N \sim 2700$ particles cm^{-3} and $\lambda_m = 6198\ s^{-1}$).

In a droplet cluster, there exists a locally high droplet number density (above the mean value), which results in relatively short interarrival times. Although droplet clustering occurs even in steady sprays as a consequence of the random character of the droplet flux, in this discussion, the term "clustering" applies to those situations for which the interarrival times differ in a *statistically significant* fashion from steady Poisson statistics. Furthermore, since these statistics are derived from temporally resolved single point observations, clustering is used in the temporal sense. As an example of such clustering, it is apparent in the histogram of Fig. 5 class (b) that the probability density of the short interarrival times is increased (relative to that which would exist given steady Poisson statistics at the same mean intensity) with a concomitant reduction in the occurrence rate of the longer time scales. Without further analysis, a

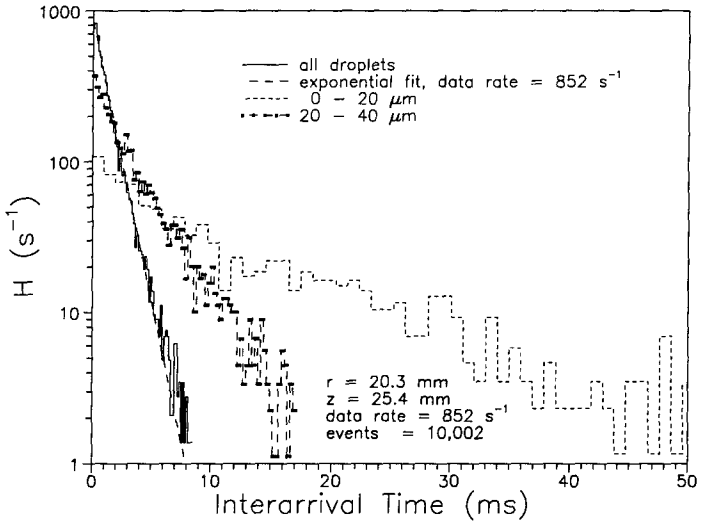

FIG. 6. Probability distribution of interarrival times for different diameter-based size classes at z = 25.4 mm and r = 20.3 mm.

distinction cannot be made between clustering that is associated with (1) closely spaced droplets traveling nominally at the same velocity and (2) droplets traveling at different velocities yet passing through the measurement volume at short time intervals (in this case, the droplets do not remain in close proximity over a significant time interval).

At the axial location z = 10 mm [corresponding to the class (b) data of Fig. 5], the maximum degree of unsteadiness, as measured by the departure from linearity of the ln $H(\tau)$ data, occurred at a radial position located roughly midway between the spray centerline and spray boundary, whereas, for the class (c) results, all the interarrival-time histograms exhibited steady behavior throughout the entire range of radial positions. Thus, droplet clustering was most intense near the shear layer (in the region that lies between the spray boundary and recirculating gases toward the center of the spray) and was limited to the smaller droplets. It is expected that only the smallest droplets, having relatively small Stokes (*St*) numbers, follow the gas-phase turbulence, and the larger droplets with high momentum and large *St* tend to be unaffected by the gas-phase flow. This correlation with *St* is consistent therefore with a clustering mechanism for which only the smallest of droplets are swept by recirculating eddies formed in the shear layer. Such droplet-laden eddies interact with the main part of the spray to produce a fluctuating and hence unsteady occurrence of smaller droplets, which interact with the droplets coming directly from the nozzle. The existence of a bimodal size distribution (attributed to the recirculation of smaller droplets into the main droplet stream coming directly from the nozzle) further supports the assertion that unsteady interarrival-time statistics occur in the shearing region as a result of eddy transport of smaller droplets.

The interarrival-time histograms for the three size classes [(a), (b), and (c)] are presented in Fig. 6 for data obtained downstream near the spray boundary at the coordinates z = 25.4 mm, r = 20.3 mm. At this position, the droplet number density was 430 particles cm^{-3}, with droplets ranging in size from 10 to 90 μm in diameter. Also presented is the exponential distribution based on the measured average intensity of 852 s^{-1} (straight dashed line). The histogram corresponding to case (b) of Fig. 6 indicates some unsteadiness for the 0–20-μm-diameter droplets, although the departure from linearity of this histogram is less than the case (b) result of Fig. 5 taken at z = 10 mm and r = 6.4 mm. This result provides additional evidence of spatial inhomogeneity in the droplet arrival-time statistics. Inspection of Fig. 6 reveals also that the histograms corresponding to cases (a) and (c) are nearly linear and conform with steady Poisson statistics. Furthermore, the measured distribution of case (a) is accurately reproduced [with Eq. (2)] using the measured average intensity. The linearity of the case (a) data indicates that the nonsteady behavior associated with the smaller droplets was masked by the relatively abundant larger droplets.

Summary

The transport of fuel droplets in a kerosene pressure-atomized spray flame was investigated using phase-Doppler interferometry to measure droplet size, velocity, and arrival time at selected axial and radial positions within the spray. Along the spray centerline and near the spray boundary, the droplet axial velocities were found to correlate with droplet diameter; i.e., higher velocities were associated with the largest droplets. Negative axial velocities (con-

sisting mostly of smaller recirculated droplets) were observed near the centerline and attributed to recirculation patterns induced by the swirling air.

Analysis of the time-series data indicated that droplet arrival is random and consistent with Poisson statistics. Steady interarrival-time statistics were obtained for the larger droplets within and external to the spray boundary. Toward the internal shear layer separating the spray and recirculated air, significant nonsteady statistical behavior was observed for the smaller droplets. The results suggest the occurrence of a clustering mechanism resulting from droplet entrainment by eddy structures formed in the shear layer. In general, these findings illustrate that it is very important to segregate the spray into size classes because of the strong dependence of such transport mechanisms on droplet diameter.

Acknowledgments

The authors acknowledge the partial support of this work by the U.S. Department of Energy, Conservation and Renewable Energy, Office of Industrial Processes, Advanced Industrial Concepts Division. Messrs. Neil Rossmeissl and Marvin Gunn are the project monitors. The work of CTA was supported by the New York State Center for Hazardous Waste Management (Dr. Ralph R. Rumer, Director). The technical assistance of Messrs. Michael J. Carrier and James D. Allen is greatly appreciated.

REFERENCES

1. Presser, C., Gupta, A. K., Avedisian, C. T., and Semerjian, H. G., *Twenty-Third Symposium (International) on Combustion*, The Combustion Institute, Pittsburgh, 1991, pp. 1361–1367.
2. Bachalo, W. D., and Rudoff, R. C., in *Liquid Particle Size Measurement Techniques*, ASTM STP 1083 (E. D. Hirleman, W. D. Bachalo, and P. G. Felton, Eds.), American Society for Testing and Materials, Philadelphia, 1990, Vol. 2, pp. 209–224.
3. Reitz, R. D., in *Liquid Particle Size Measurement Techniques*, ASTM STP 1083 (E. D. Hirleman, W. D. Bachalo, and P. G. Felton, Eds.), ASTM, Philadelphia, 1990, Vol. 2, pp. 225–237.
4. Edwards, C. F., and Rudoff, R. C., *Twenty-Third Symposium (International) on Combustion*, The Combustion Institute, Pittsburgh, 1990, pp. 1353–1359.
5. Bulzan, D. L., Levy, Y., Aggarwal, S. K., and Chitre, S., *Atomiza. Sprays* 2(4):445–462 (1992).
6. Presser, C., and Gupta, A. K., AIAA 93–0132, *31st AIAA Aerospace Sciences Meeting*, Reno, NV, 1993.
7. Presser, C., and Gupta, A. K., in *Heat Transfer in Fire and Combustion Systems* (B. Farouk, M.P. Menguc, R. Viskanta, C. Presser, and S. Chellaiah, Eds.), ASME, New York, 1993, HTD-Vol. 250, pp. 79–92.
8. Presser, C., Gupta, A. K., and Semerjian, H. G., *Combust. Flame* 92:25–44 (1993).
9. Presser, C., Gupta, A. K., Semerjian, H. G., and Avedisian, C. T., *J. Propul. Power* 10:631 (1994).
10. Gupta, A. K., Presser, C., Hodges, J. T., and Avedisian, C. T., AIAA 94-0115, *32nd Aerospace Sciences Meeting*, Reno, NV, 1994.
11. Zurlo, J. R., Presser, C., and Gupta, A. K., *Atomiza. Sprays*, in review.
12. Edwards, C. F., and Marx, K. D., *6th Annual Conference on Liquid Atomization and Spray Systems (ILASS Americas '93)*, Worcester, MA, 1993, pp. 245–259.
13. Edwards, C. F., and Marx, K. D., Paper No. 93-082, Western States Section—Combustion Institute, 1993 Fall Meeting, Menlo Park, CA.
14. Snyder, D. L., *Random Point Processes*, John Wiley, New York, 1975.

COMMENTS

J. A. Bossard, Arizona State University, USA. What are some of the implications of your work in addressing the discrepancies that exist between temporal measurements (i.e., the PDPA) and spatial measurements (i.e., PIV), particularly with regard to differences in measured number density and volume flux?

Author's Reply. For temporal-based measurements of droplet number density and volume flux, the functional form of the interarrival time distribution function must be known in order to account properly for statistical biases in the raw data. Specifically, with knowledge of the interarrival statistics and effective probe volume dimensions, droplet number density and volume flux can be determined from droplet velocity and diameter measurements. Yet the results of this work demonstrate that in real sprays, droplet interarrival times (especially for the smallest droplets) do not always follow steady Poisson statistics. Consequently, given a situation for which the arrival time statistics are unsteady, a priori assumption of statistically steady behavior is not justified and will lead to erroneous estimates of measured number density and volume flux. It is thus possible that some discrepancies between temporal and spatial measurements may be attributed to the failure to account properly for unsteadiness in the interarrival time statistics of droplets or tracer particles. In an analogous fashion, one must know the interparticle distance distribution function when determining number density and volume flux from

spatial measurements. The occurrence of statistically significant *spatial* clustering would need to be accounted for in the determination of droplet number density and volume flux from such data.

•

Joseph J. Sangiovanni, United Technologies Research Center, USA. Does your data analysis properly account for droplet coalescence? For example, when small, faster moving droplets collide with larger, slower moving droplets. If droplet coalescence is accounted for, can you then quantify coalescences by analysis of droplet arrival time statistics as functions of droplet size, number density, and position?

Author's Reply. Droplet coalescence does not explain the unsteadiness in the measured interarrival time statistics. As discussed in the text, the minimum mean interdroplet spacing is relatively large so that droplet collision is a rare event. Furthermore, even in the densest region of the spray (where the likelihood of droplet collision is highest), the arrival time statistics remained steady. Unsteadiness in the statistics was observed only in the relatively dilute spray interior. Finally, the unsteady behavior was associated with only the smaller-sized droplets. However, as suggested in your question, collisions would tend to occur between smaller- and larger-sized droplets. Consequently, a collision-induced departure from steady statistics would be expected for small and large droplets. Since only the smallest droplets exhibited unsteady behavior, droplet coalescence does not then explain satisfactorily the occurrence of statistical unsteadiness.

Coalescence would influence the occurrence rate within any size class of droplets that are undergoing collisions. One could model the probability of droplet coalescence to quantify its effect on the form of the interarrival time distribution. For example, with no correlation between droplet arrival time and the collision probability (for droplets within a sufficiently narrow size class), coalescence events would be randomly distributed among these droplets. As a result, the form of the interarrival time distribution for such a size class would remain unaffected by collisions. Consequently, droplet coalescence may not necessarily result in unsteady interarrival time statistics. Nevertheless, droplet coalescence would tend to increase the number of larger droplets and concurrently deplete the relative abundance of smaller-sized droplets. An increase in the occurrence rate of larger droplets proceeding in the downstream direction might provide some evidence of droplet coalescence since droplet evaporation and deceleration tend to reduce the droplet occurrence rate.